

In Vivo Pretargeting Based on Cysteine-selective Antibody Modification with IEDDA Bioorthogonal Handles for Click Chemistry

Vera F. C. Ferreira¹, Bruno L. Oliveira^{2*}, Alice D'Onofrio¹, Carlos M. Farinha³, Lurdes Gano^{1,4}, Ant3nio Paulo^{1,4}, Gonçalo J. L. Bernardes^{2,5*}, Filipa Mendes^{1,4*}

¹ Center for Nuclear Sciences and Technologies (C²TN), Instituto Superior T3cnico, Universidade de Lisboa, Estrada Nacional 10, 2695-066 Bobadela LRS, Portugal

² Instituto de Medicina Molecular Jo3o Lobo Antunes (iMM-JLA), Faculdade de Medicina, Universidade de Lisboa, Av. Prof. Egas Moniz, 1649-028 Lisboa, Portugal

³ Biosystems and Integrative Sciences Institute (BioISI), Faculdade de Ci3ncias, Universidade de Lisboa, Campo Grande, 1749-016 Lisboa, Portugal

⁴ Departamento de Engenharia e Ci3ncias Nucleares (DECN), Instituto Superior T3cnico, Universidade de Lisboa, Estrada Nacional 10, 2695-066 Bobadela LRS, Portugal

⁵ Department of Chemistry, University of Cambridge, Lensfield Road, CB2 1EW Cambridge, United Kingdom

KEYWORDS. Protein modification, Bioconjugation, Pretargeting, IEDDA reaction, carbonylacrylic reagents.

ABSTRACT: Pretargeted imaging has emerged as an effective multi-step strategy aiming to improve imaging contrast and reduce patient radiation exposure through decoupling of the radioactivity from the targeting vector. The inverse electron-demand Diels-Alder (IEDDA) reaction between a *trans*-cyclooctene (TCO)-conjugated antibody and a labelled tetrazine holds great promise for pretargeted imaging applications due to its bioorthogonality, rapid kinetics under mild conditions, and formation of stable products. Herein, we describe the use of functionalized carbonylacrylic reagents for site-specific incorporation of TCO onto an human epidermal growth factor receptor 2 (HER2) antibody (THIOMAB) containing an engineered unpaired cysteine residue, generating homogeneous conjugates. Precise labelling of THIOMAB-TCO with a fluorescent or radiolabelled tetrazine revealed the potential of the TCO-functionalized antibody for imaging the HER2 after pretargeting in a cellular context in a HER2 positive breast cancer cell line. Control studies with MDA-MD-231 cells, which do not express HER2, further confirmed the target specificity of the modified antibody. THIOMAB-TCO was also evaluated *in vivo* after pretargeting and subsequent administration of an ¹¹¹In-labelled tetrazine. Biodistribution studies in breast cancer tumor-bearing mice showed a significant activity accumulation on HER2⁺ tumors, which was 2.6-fold higher than in HER2⁻ tumors. Additionally, biodistribution studies with THIOMAB without the TCO handle also resulted in a decreased uptake of ¹¹¹In-DOTA-Tz on HER2⁺ tumors. Altogether, these results clearly indicate the occurrence of the click reaction at the tumor site, *i.e.*, pretargeting of SK-BR-3 HER2-expressing cells with THIOMAB-TCO and reaction through the TCO moiety present in the antibody. The combined advantages of site-selectivity and stability of TCO tagged-antibodies could allow application of bioorthogonal chemistry strategies for pretargeting imaging with minimal side-reactions and background.

Introduction

Specific binding of antibodies to a given target with nano- or picomolar affinity has provided the basis for developing highly sensitive, antibody-based imaging agents to assess disease in preclinical and clinical studies. Indeed, there are currently over 30 clinical trials evaluating the utility of immuno-nuclear imaging agents in multiple cancer types.^{1,2}

However, despite their attractive properties, antibodies present a few limitations that hamper their use as imaging agents, namely a long serum half-life (1-3 weeks).³ As several days are required to achieve high imaging contrast, antibodies are commonly labelled with long-lived radionuclides, such as zirconium-89 (⁸⁹Zr, $t_{1/2}$ = 78.4 hr), copper-64 (⁶⁴Cu, $t_{1/2}$ = 12.7 hr), iodine-

124 (^{124}I , $t_{1/2} = 100.3$ hr) and yttrium-86 (^{86}Y , $t_{1/2} = 14.7$ hr)⁴, translating in prolonged patient radiation exposure.³

An alternative approach arose with the development of the pretargeting strategy, based on the decoupling of the radioactivity from the targeting vector.^{5,6} This strategy relies on the combination of two components, a targeting vector and a posteriorly administered, low molecular weight radioligand which leads to *in vivo* radiolabelling. The pretargeting strategy combines the high affinity and specificity of the vector, usually antibody-based, to the target, and the superior pharmacokinetic properties of the radioligand. The separate administration of the targeting vector and radioligand allows the use of short-lived radionuclides, reduces the patient radiation exposure with minimization of the radiation dose delivered to non-target organs and tissues, and improves the imaging contrast at earlier time points.^{7,8} Bioorthogonal reactions have emerged as promising tools to selectively modify biological molecules in order to investigate cellular functions and dynamic processes in living systems without interfering with those processes.^{9,10} One of the most developed applications of bioorthogonal reactions has been in the pretargeted imaging through the assembly of molecular imaging agents *in vivo*.¹¹ To date, the inverse electron-demand [4+2] Diels-Alder (IEDDA) cycloaddition, between a 1,2,4,5-tetrazine and strained alkene dienophile, is considered the most suitable click reaction to pretargeted imaging applications, as it presents high selectivity and fast kinetics, proceeds in mild conditions, and is catalyst-free.¹² The IEDDA reaction has been applied in *in vivo* pretargeted imaging using a variety of radionuclides, as technetium-99m ($^{99\text{m}}\text{Tc}$, $t_{1/2} = 6.0$ hr)¹³, indium-111 (^{111}In , $t_{1/2} = 67.2$ hr)¹⁴,¹⁵, copper-64 (^{64}Cu , $t_{1/2} = 12.7$ hr)¹⁶⁻¹⁸, fluorine-18 (^{18}F , $t_{1/2} = 109.8$ min)¹⁹⁻²¹ and gallium-68 (^{68}Ga , $t_{1/2} = 68.0$ min)²²⁻²⁴.

Conjugation of IEDDA reactant moieties to antibodies usually relies on amine-reactive *N*-hydroxysuccinimide (NHS) esters for covalent binding.¹⁵ This strategy leads to random conjugation of IEDDA partners to lysine residues resulting in heterogeneous conjugates with undefined composition, which can substantially lower the bioactivity of the modified protein and lead to unpredictable *in vivo* behaviour. It is therefore critical to establish a well-defined conjugation strategy for antibody modification to ensure that both targeting and pharmacokinetics are maintained.

Site-selective protein modification methods have been crucial for the development of new biologically active protein conjugates for *in vivo* applications.²⁵ From all the natural amino acids, cysteine is considered the ideal amino acid for selective protein modification due to its low abundance and the high nucleophilicity of the sulfhydryl side chain.^{26,27} Ma-

leimides are still the most commonly used reagents for cysteine bioconjugation. These reagents present fast reaction kinetics in aqueous media and are easy to chemically-modify. However, it is known that the thio-succinimidyl conjugates formed are unstable and react with thiols present in plasma, leading to maleimide release.²⁸⁻³⁰

Recently, we reported a new methodology for irreversible cysteine-selective protein bioconjugation *via* carbonylacrylic reagents.^{31,32} These easily-prepared reagents are highly reactive for cysteine in aqueous conditions at near neutral pH and using stoichiometric amounts, and form stable products that remain biologically functional. The aforementioned characteristics in combination with the availability of biologically relevant cysteine-tagged proteins make this method suitable for routine preparation of well-defined and stable conjugates for chemical biology applications.

Herein, a novel carbonylacrylic derivative functionalized with a *trans*-cyclooctene (TCO) moiety was developed and conjugated to TH10MAB™ LC-V205C, a modified trastuzumab antibody against the human epidermal growth factor receptor 2 (HER2) presenting an engineered cysteine in the light chain.³³ This receptor has already been exploited in clinical imaging of breast and gastric cancer HER2-expressing tumors.^{14, 19, 20, 34-40} Pretargeting was firstly explored *in vitro* to assess the IEDDA reaction between the antibody bound to HER2-expressing cells and a fluorescent/radiolabelled tetrazine. Then, *in vivo* studies were performed in a relevant HER2+ mouse model using an ^{111}In -labelled tetrazine. This approach represents the first maleimide-free methodology for cysteine-based incorporation of TCO onto antibodies for IEDDA pretargeting approaches.

Cysteine-selective antibody modification

A TCO-functionalized carbonylacrylic reagent for cysteine-antibody modification was synthesized as depicted in **Figure 1**. Activation of the commercially available 3-benzoylacrylic acid was performed using pentafluorophenyl trifluoroacetate as activating agent to give compound **1** (**Figure 1a i**). Subsequent introduction of a short polyethylene glycol (PEG) linker to increase hydrophilicity was accomplished by reacting precursor **1** with *t*Bu-NH-PEG₅-(CH₂)₂-NH₂, followed by *tert*-butyl deprotection with trifluoroacetic acid (TFA) (**Figure 1a ii-iii**). Finally, reaction of the PEGylated compound **3** with the commercially available TCO-NHS-ester yielded the water-soluble, TCO-functionalized reagent **CA-TCO** (carbonylacrylic-TCO), with an overall yield of ~ 28% (**Figure 1a iv** and **Figures S1-S3**).

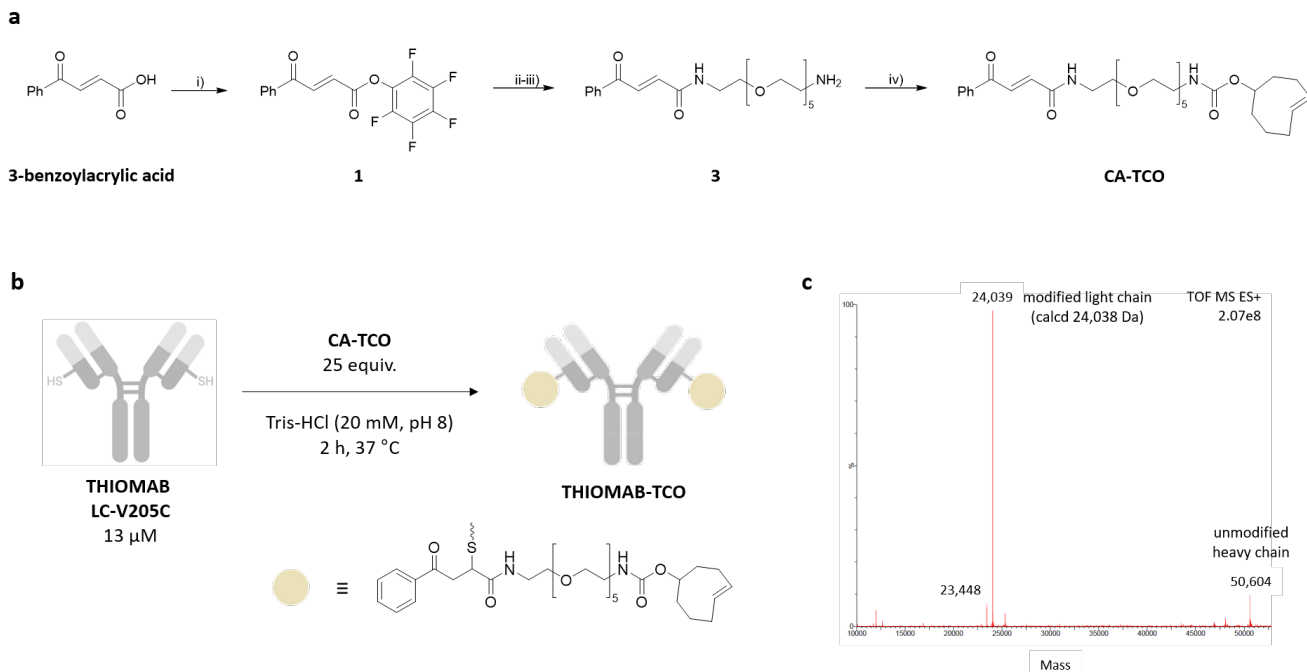


Figure 1: Carbonylacrylic-TCO reagent for antibody modification. (a) Synthesis of carbonylacrylic derivative functionalized with TCO. i) 3-benzoylacrylic acid, 1.1 equiv. pentafluorophenyl trifluoroacetate, 2 equiv. DIPEA, anhydrous DCM, RT, 2 h, η = 68.4%; ii) 1.1 equiv. *t*Bu-NH-PEG₅-(CH₂)₂-NH₂, 2 equiv. DIPEA, anhydrous DCM, RT, 1 h, η = 82.9%; iii) TFA, DCM, RT, 1 h; iv) TCO-NHS-ester, 1.5 equiv. **3**, 2 equiv. DIPEA, anhydrous DCM, RT, overnight, η = 50.6%. Ph – phenol; **(b)** Schematic overview of antibody modification *via* reaction with CA-TCO (2 h at 37 °C in Tris-HCl buffer); **(c)** ESI-MS spectrum of THIOMAB after reaction with CA-TCO.

The efficacy of CA-TCO for site-selective protein modification was tested using the anti-HER2 antibody THIOMAB LC-V205C.³³ Bioconjugation proceeded to completion (> 95%) upon reaction with 25 equivalents of CA-TCO for 2 h at 37 °C. The antibody was treated with the reducing agent tris(2-carboxyethyl)phosphine (TCEP) prior to mass spectrometry analysis to reduce the interchain disulfide bridges, yielding the light and heavy chains. Liquid chromatography-mass spectrometry (LC-MS) analysis after TCEP reduction showed a single modification in the light chain, while the heavy chain remained unmodified (**Figure 1c** and **Figures S4 – S6**), resulting in two TCO molecules per each THIOMAB molecule. This result demonstrates that the IEDDA-functionalized carbonylacrylic reagent retains the selectivity for cysteine, and therefore can be used for site-selective modification of proteins of interest.

Precise antibody fluorescent labelling

To demonstrate the applicability of the TCO-functionalized carbonylacrylic reagent to fluorescently label proteins, the THIOMAB-TCO conjugate was reacted with a fluorescent

(Tz-Cy3, **Figure 2a** and **Figure S7**) and non-fluorescent (benzylamino methyl-tetrazine, **Figure S8**) tetrazine. Mass spectrometry analysis indicated complete conversion of THIOMAB-TCO to the corresponding antibody conjugates (**Figure 2** and **Figure S6**) resulting in the incorporation of two tetrazine moieties per antibody. SDS-PAGE in-gel fluorescence analysis of the reaction revealed fluorescent labelling by click reaction between the TCO moiety present in each light chain of the antibody and the fluorescent tetrazine, indicated by the ~25 kDa fluorescent band (**Figure 2c**). A fluorescent band of ~ 50 kDa was also observed, that might correspond to the formation of a dimer between the modified light chains, as there was no indication of conjugation to the heavy chain (~ 50 kDa) by mass spectrometry. In fact, dimerization of the light chains was also observed by LC-MS analysis performed under strong denaturing conditions (*i.e.*, TCEP reduction, acetonitrile as running solvent, desolvation temperature 400 °C, **Figures S7** and **S8**). Importantly, nonspecific binding of the tetrazine fluorophore to the heavy chain was also not observed by SDS-PAGE (**Figure S9**).

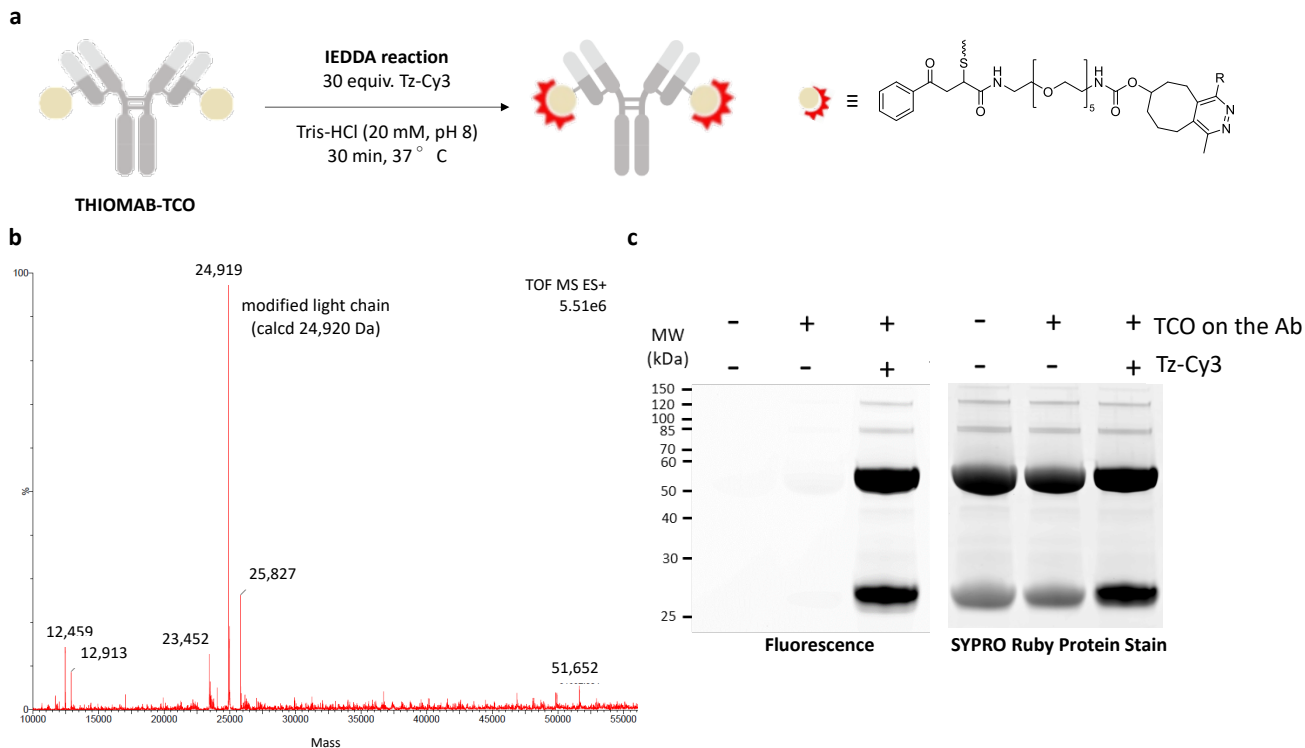


Figure 2: Fluorescent labelling studies of THIOMAB-TCO. (a) Schematic overview of antibody labelling *via* click reaction with 6-methyl-tetrazine-sulfo-Cy3 (Tz-Cy3); (b) ESI-MS spectrum of THIOMAB-TCO after reaction with fluorescent tetrazine (30 min at 37 °C in Tris-HCl buffer); (c) SDS-PAGE analysis of fluorescent labelling of THIOMAB-TCO conjugate. Proteins were resolved in a 4 - 12% gradient NuPAGE Bis-Tris mini gel under reducing conditions, and revealed using SYPRO Ruby staining.

***In vitro* cellular pretargeting *via* click reaction of antibody conjugate with a fluorescent IEDDA partner**

Proven the efficacy of the TCO-functionalized carbonylacrylic derivative to create a precisely modified, fluorescently labelled antibody through TCO-functionalization, the next step was to assess if the antibody conjugate could be used in a pretargeting approach. With this purpose, the human breast cancer SK-BR-3 cells (HER2+, 3+ immunohistochemistry (IHC) score) and the triple-negative MDA-MB-231 (HER2-) cells⁴¹ were pretargeted with THIOMAB-TCO followed by treatment with the fluorescent tetrazine Tz-Cy3 (Figure 3a). HER2 visualization at the plasma membrane of SK-BR-3 cells through confocal microscopy indicated successful click reaction between the TCO moiety present on THIOMAB-TCO and the fluorescent tetrazine in cell medium, evidencing the bioorthogonality of the IEDDA reaction (Figure 3b). Importantly, no fluorescent signal was detected at the plasma membrane of SK-BR-3 cells treated with tetrazine only and pretargeted with the unmodified THIOMAB (Figure S10).

These results clearly indicate that the fluorescent signal is associated with the labelling of the antibody *via* TCO. Lastly, confocal imaging of the HER2- cell line further support labelling of the HER2 receptor, as no fluorescence was detected at the cell surface of MDA-MB-231 cells treated with THIOMAB-TCO followed by Tz-Cy3 (Figure 3b). Staining of SK-BR-3 cells treated with THIOMAB-TCO was also observed by flow cytometry after reaction with Tz-Cy3 (Figure 3c and Figure S11), confirming IEDDA reaction between the TCO moiety present in THIOMAB-TCO and tetrazine. Cell staining was antibody-associated, as shown by the low unspecific binding of Tz-Cy3 to SK-BR-3 cells (~10%). Blocking of HER2 receptors with unmodified THIOMAB before incubation with THIOMAB-TCO led to a decrease in the fluorescence intensity observed in SK-BR-3 cells (~7% binding after blocking), supporting that THIOMAB-TCO retained its specificity for HER2. The high percentage of stained SK-BR-3 cells (~73%) vs. stained MDA-MB-231 cells (~8%) further indicated that binding of THIOMAB-TCO was specific for HER2.

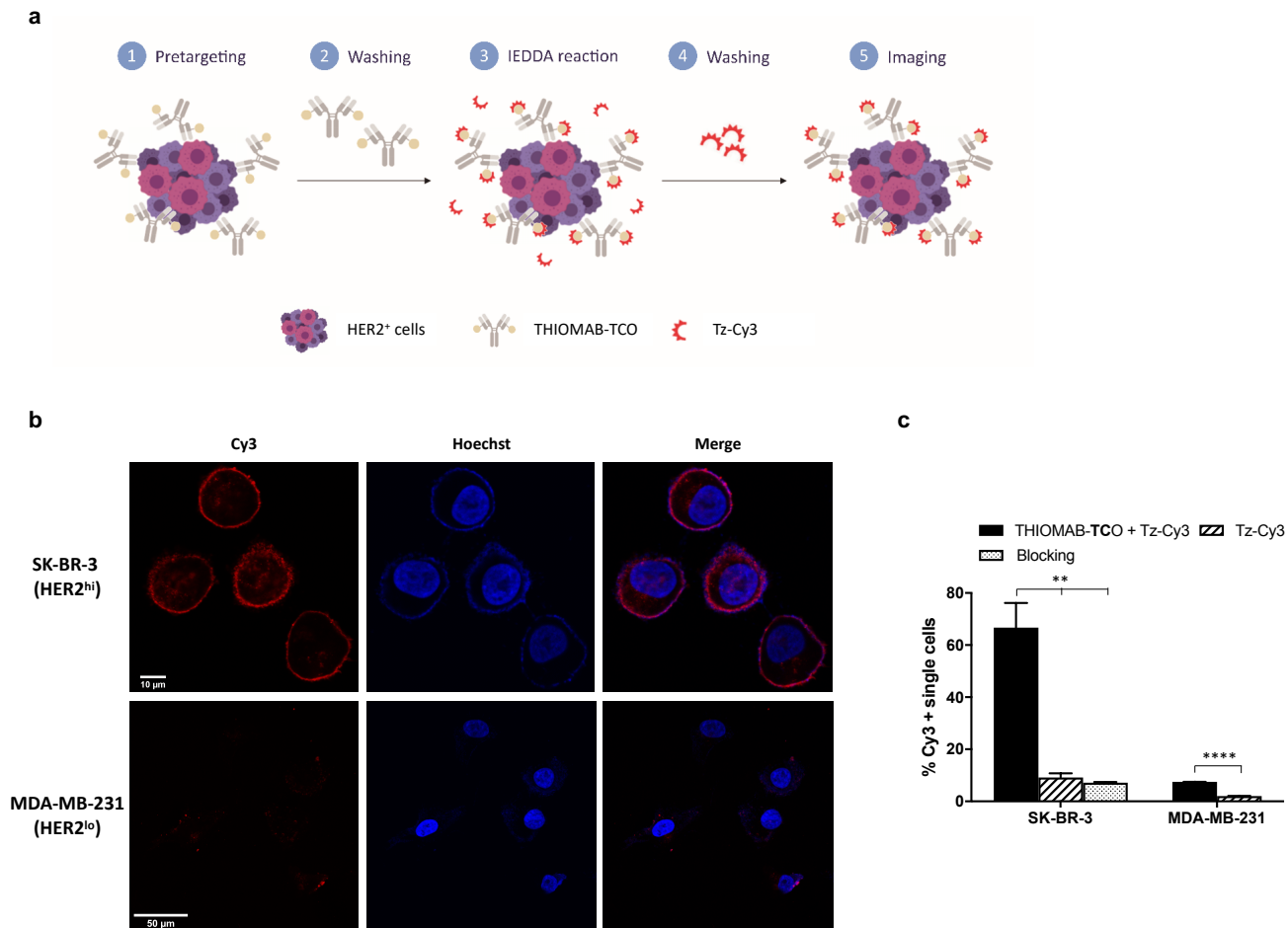


Figure 3: Pretargeted cell labelling with THIOMAB-TCO. (a) Schematic overview of pretargeting strategy; (b) Confocal images of SK-BR-3 and MDA-MB-231 cells pretargeted with THIOMAB-TCO for 45 min at 37 °C followed by treatment with Tz-Cy3 for 30 min at 37 °C. Nuclei are shown in blue. Experiments performed in triplicate; (c) Percentage of Cy3-positive single cells from the cell population in SK-BR-3 and MDA-MB-231 cells treated with THIOMAB-TCO (45 min, RT), blocking with THIOMAB (45 min, RT) before THIOMAB-TCO, followed by treatment with Tz-Cy3 (30 min, 37 °C), and Tz-Cy3 only. Statistical analysis was performed with two-way ANOVA, with p -value < 0.05 considered as the level of statistical significance.

Altogether, the results obtained by confocal microscopy and flow cytometry demonstrate *in vitro* pretargeting of HER2-expressing cells with THIOMAB-TCO in a cellular context. Moreover, the results also indicate that the THIOMAB-TCO conjugate retained the specificity for its target after TCO functionalization, being able to detect HER2 at the surface of HER2-expressing cells after local reaction with a fluorescent tetrazine.

Precise antibody radiolabelling

Considering the successful *in vitro* pretargeting of HER2-expressing cells, the work proceeded with the study of THIOMAB-TCO for *in vivo* pretargeting through IEDDA reaction with a radiolabelled tetrazine. With this purpose, the chelating agent 1,4,7,10-tetraazacyclododecane-1,4,7,10-tetraacetic acid (DOTA) functionalized with a tetrazine moiety⁴² was labelled with ¹¹¹In by reaction with ¹¹¹InCl₃ for 15 min at 80 °C in 0.1 M ammonium acetate buffer pH 7 (Figure

4a). After HPLC purification, ¹¹¹In-DOTA-Tz was isolated with a radiochemical purity (RCP) $> 95\%$ and a radiochemical yield ranging from 44 to 56% (Figure 4b). Analysis by instant thin layer chromatography (iTLC) discarded the formation of indium colloids (Figure S12). THIOMAB-TCO was then radiolabelled by click reaction with the purified ¹¹¹In-DOTA-Tz for 5 min at 37 °C, with ~92% of the activity being associated to the clicked antibody (Figure 4c) (RCP $> 99\%$ after purification, Figure S13). These results further confirm the fast kinetics and high efficiency of the biorthogonal reaction, as both partners were used at very low concentration, in the micromolar range.

The ¹¹¹In-labelled antibody remained fully stable in cell culture medium and was totally resistant to transchelation in the presence of the In-111 chelating agent diethylenetriamine pentaacetic acid (DTPA, incubation at 37 °C for 3 h, Figure S14). Finally, in human serum, a time-dependent decrease in the radiochemical stability of the tetrazine-TCO

antibody was observed (~54% of RCP after 24 h of incubation at 37 °C) (**Figure S15**).

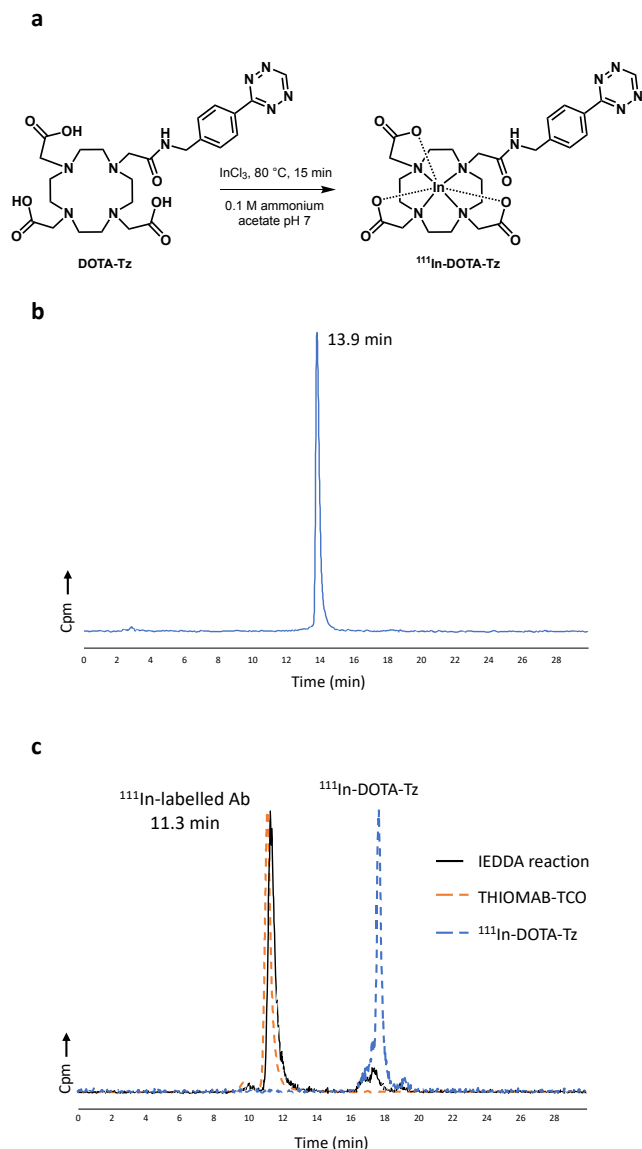


Figure 4: Radiolabelling of THIOMAB-TCO. (a) Labelling of DOTA-Tz ($[1 \times 10^{-4} \text{ M}]$) with ^{111}In for 15 min at 80 °C; (b) Characterization of $^{111}\text{In-DOTA-Tz}$ by RP-HPLC after purification; (c) SE-HPLC analysis of IEDDA reaction of THIOMAB-TCO with $^{111}\text{In-DOTA-Tz}$ for 5 min at 37 °C (black line, γ -detection). Orange dashed line represents analysis of THIOMAB-TCO (UV detection) and blue dashed line analysis of $^{111}\text{In-DOTA-Tz}$ (γ -detection). Cpm – counts per minute.

***In vitro* pretargeting of HER2-positive cells for HER2 imaging**

Proven the ability to rapidly radiolabel THIOMAB-TCO with ^{111}In in mild conditions through the IEDDA reaction, an *in vitro* pretargeting approach was explored. HER2+ and HER2- cells were pretargeted with THIOMAB-TCO followed

by treatment with $^{111}\text{In-DOTA-Tz}$ (**Figure 5a**). Low unspecific binding of the radiolabelled tetrazine was observed for SK-BR-3 cells (0.1-0.2%).

Click reaction between HER2-bound THIOMAB-TCO and $^{111}\text{In-DOTA-Tz}$ was observed in SK-BR-3 cells after 10 min of incubation with the radiolabelled tetrazine, with a significantly higher uptake in SK-BR-3 cells when compared to controls (*e.g.*, bound activity to MDA-MB-231, **Figure 5a**, p -value <0.0001).

Similarly, as previously observed for the fluorescent tetrazine, blocking of HER2 receptors with unmodified THIOMAB (**Figure 5b**) resulted in a 3.7 fold decrease in the uptake of pretargeted SK-BR-3 cells at 180 min of incubation (p -value <0.0001). It is worth to mention that a significant time-dependent increase of the uptake in the pretargeted SK-BR-3 cells was observed after 30 min of incubation. This behavior was also observed in SK-BR-3 cells treated with the already clicked antibody, which was allowed to bind to HER2 over time (**Figure S16**). Considering that the click reaction occurs within 5 min of incubation in cell medium, the increase in the uptake over time might be explained not by a late click reaction, but by internalization of the THIOMAB-TCO-HER2 complexes and posterior recycling to the membrane, where THIOMAB-TCO is again available to react with free $^{111}\text{In-DOTA-Tz}$ present in the assay medium. This hypothesis is supported by confocal immunofluorescence microscopy studies in SK-BR-3 cells in which the internalized trastuzumab was detected after 3 h at 37 °C.⁴³ Additionally, a recent study demonstrated that trastuzumab-HER2 complexes internalize both in HER2^{high} level and HER2^{low} level cells, but present distinct post-endocytic trafficking behavior, dependent on the expression levels of HER2.⁴⁴ In HER2^{hi} cells, internalized trastuzumab traffics to early endosomes and remains on the limiting endosomal membrane, while an only small fraction of antibody-HER2 complexes enters the lysosomal pathway. The trastuzumab is then expected to be segregated from these endosomes into the endocytic recycling pathway.⁴⁴ By contrast, in HER2^{lo} cells, internalized antibody-HER2 complexes enter the lysosomal pathway, as there are no evidences of trastuzumab recycling to the membrane.⁴⁴ The uptake results obtained in pretargeted MDA-MB-231 cells are also in agreement with the proposed trafficking model. Internalization and lysosomal degradation of THIOMAB-TCO-HER2 complexes might have diminished the THIOMAB-TCO available to react with $^{111}\text{In-DOTA-Tz}$, which was reflected in a similar percentage of cell-bound activity over time ($0.3\% \pm 0.1$ at 5 min vs. $0.6\% \pm 0.1$ at 180 min), comparable to the unspecific binding of the radiolabelled tetrazine (0.3 ± 0.1 at 5 min vs. $0.4\% \pm 0.1$ at 180 min).

***In vivo* pretargeting of HER2-positive tumours**

We next evaluated the pretargeting strategy using a human HER2 tumor xenograft mouse model. Biodistribution of ^{111}In -DOTA-Tz was assessed after pretargeting with THIOMAB-TCO followed by intravenous injection of ^{111}In -DOTA-Tz 24 h later. Biodistribution in the organs was evaluated at 24 h post-injection of the tetrazine radiocomplex (**Figures 5c and 5d**).

The tumoral uptake in SK-BR-3 tumor bearing mice receiving THIOMAB-TCO was significantly higher when compared to control studies (1.02% vs. 0.39% and 0.33% of injected dose (ID)/g for unmodified THIOMAB in SK-BR-3 xenografts and for THIOMAB-TCO in MDA-MB-231 xenografts respectively, p -value <0.01). These results clearly indicate click reaction at the tumor site, *i.e.*, pretargeting of HER2+ cells with THIOMAB-TCO and reaction with ^{111}In -DOTA-Tz through the TCO moiety present in the antibody.

In the overall biodistribution profile, it is clear that the majority of the activity was excreted 24 h post injection of ^{111}In -DOTA-Tz, with values ranging from 89.5 to 93.7% ID

(Table S1 and Figure S17). Unlike small molecules, antibodies are too large to be filtered by the kidneys and are not eliminated in the urine. In fact, biodistribution of ^{111}In -DOTA-Tz in normal mice revealed an excretion rate of $91.8\% \pm 1.0$ at 1 h after injection.⁴² Hence, the high excretion rate obtained with the pretargeting strategy is in agreement with the observed fast elimination of the hydrophilic ^{111}In -DOTA-Tz, which accumulated in the kidneys with values between 1.40 - 1.79% ID/g for the three groups of mice (**Figure 5c**), supporting its elimination through the renal pathway. The rapid elimination of ^{111}In -DOTA-Tz is also reflected in low uptake values in the main organs and tissues. Renal excretion was significantly lower in SK-BR-3 mice receiving THIOMAB-TCO comparing with mice treated with unmodified THIOMAB (89.5 vs. 93.7% ID, p -value <0.01, **Figure S17**), while accumulation in tumor, blood, and remaining organs was higher for THIOMAB-TCO. The activity found in the liver (0.21 - 0.59% ID/g) represents the contribution of the hepatobiliary excretion pathway, probably associated to the excretion of the clicked radiolabelled antibody.

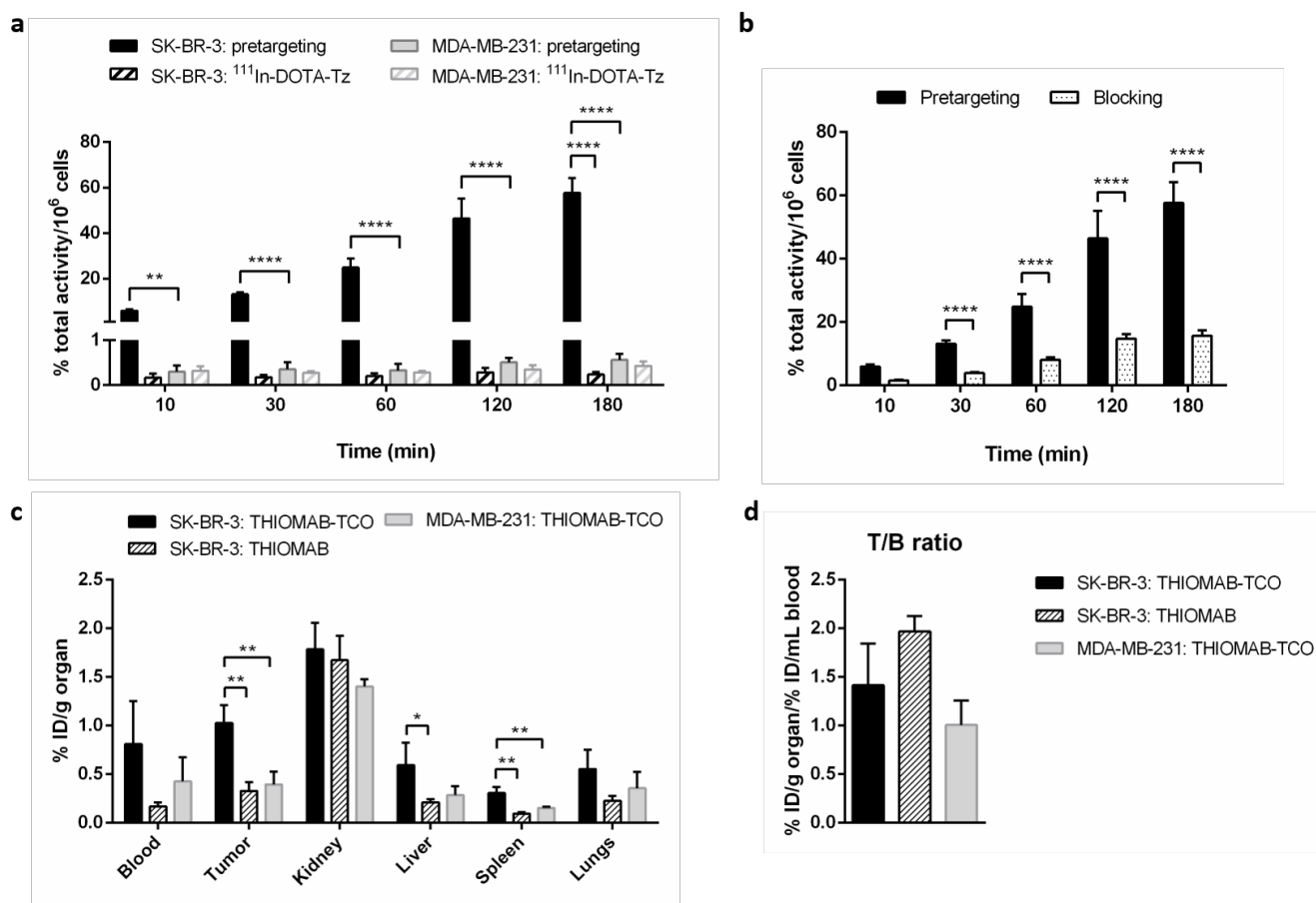


Figure 5: *In vitro* and *in vivo* pretargeting. (a) *In vitro* click reaction of THIOMAB-TCO with ^{111}In -DOTA-Tz in SK BR-3 and MDA-MB-231 cells. Cells were pretargeted with THIOMAB-TCO for 45 min at 37 °C. The medium containing the antibody-TCO was removed at different time points and cells incubated with ^{111}In -DOTA-Tz at 37 °C. For the control experiment, cells were incubated with ^{111}In -DOTA-Tz only. **(b)** Blocking of SK-BR-3 cells with THIOMAB (45 min, 37 °C) before pretargeting. Cellular uptake values are expressed as a percentage of total activity added to cells normalized per million of cells \pm standard deviation (two independent

assays with $n = 3-4$ replicates for each time point). Statistical analysis was performed with two-way ANOVA, with p -value <0.05 considered as the level of statistical significance; **(c)** Biodistribution (% ID/g) in the most relevant organs of ^{111}In -DOTA-Tz administered after pretargeting with THIOMAB-TCO, in female athymic nude mice ($n = 3$ for each group), 24 h post injection of ^{111}In -DOTA-Tz (48 h after antibody injection). Statistical analysis was performed with two-way ANOVA, with p -value <0.05 considered as the level of statistical significance; **(d)** Tumor-to-blood ratios (%ID/g organ/%ID/mL blood) of SK-BR-3 and MDA-MB-231 tumor-bearing mice receiving THIOMAB-TCO or THIOMAB, 24 h post injection of ^{111}In -DOTA-Tz (48 h after antibody injection). ID/g refers to injected dose/gram.

Higher activities were observed in the blood of SK-BR-3 and MDA-MB-231 tumor-bearing mice receiving THIOMAB-TCO comparing with mice receiving the unmodified THIOMAB (0.81 – 0.42 % vs. 0.17% ID/g, respectively) (**Figure 5c**). This difference might be associated to systemic retention of the clicked antibody. Indeed, it is well known that antibodies exhibit a relatively fast distribution phase followed by a slower elimination phase, contributing to long serum half-lives.⁴⁵ This biphasic pharmacokinetic profile might explain that, after 48 h of antibody injection, THIOMAB-TCO remained in circulation available for click reaction with ^{111}In -DOTA-Tz. The unmodified THIOMAB was also possibly in circulation, but unable of systemic click reaction due to the absence of a TCO moiety. The possibility of HER2 shedding into systemic circulation is also not discarded.

The Tumor/Blood ratios (T/B ratios) of the three mice groups ranged from 1.0 to 2.0 (**Figure 5d**). Overall, the higher systemic retention of the clicked antibody contributed to the relatively low T/B ratio observed in SK-BR-3 mice treated with THIOMAB-TCO (~ 1.4). In contrast, although the tumor uptake was lower in SK-BR-3 mice receiving THIOMAB, the absence of the TCO moiety in the antibody contributed also to a lower activity in the blood, increasing the T/B ratio to ~ 2.0 . Therefore, optimization is required to reduce the antibody blood concentration, possibly through the use of clearing agents prior to administration of the radiolabelled tetrazine.^{46, 47}

In a recent study, the pretargeting of HER2-expressing tumors was exploited through click reaction between THIOMAB antibodies containing different molar ratios of TCO moieties incorporated *via* maleimide chemistry.¹⁴ At 24 h post ^{111}In -DOTA-Tz injection, the tumoral uptake in KPL-4 (HER2+) tumor-bearing mice was 2% ID/g, ~ 2 -fold higher than the obtained in this study, at the same antibody concentration (5 mg/kg) and using comparable injected doses (~ 3.5 MBq of ^{111}In -DOTA-Tz in this study vs. 18.5 MBq). The discrepancy in the tumoral uptake might be related with the different HER2-expressing cell line used.

HER2 is a highly-expressed, internalizing target that is passively recycled to the plasma membrane after endocytosis.⁴⁴ Internalization of the TCO-modified antibody with its target could constitute a limitation to the pretargeting approach

since ^{111}In -DOTA-Tz is not able to cross the cellular membrane due to the polar/charged nature of the metal/chelate moiety. Hence, internalization of THIOMAB-TCO might contribute to the low tumoral uptake in SK-BR-3 tumor-bearing mice, as the HER2-bound antibody was not always available at the cell surface to react with ^{111}In -DOTA-Tz. In fact, the cellular uptake results presented here with pretargeted SK-BR-3 cells support the internalization of THIOMAB-TCO-HER2 complexes, with a subpopulation recycling back to the membrane.

Recently, the bioavailability of HER2 at the cell surface was shown to be modulated through a caveolin 1 (CAV1)-mediated mechanism.^{48, 49} Indeed, CAV1 depletion by treatment with lovastatin was shown to increase HER2 half-life and availability at the cell membrane in HER2-positive tumors (*e.g.*, NCIN87 cells). Importantly, the SK-BR-3 cells used in this study do not form caveolae as they lack caveolin 1.⁵⁰ The use of a statin, however, might work by modulating other endocytic trafficking systems.⁵¹ Therefore, pharmacological treatment with lovastatin is also envisaged in future biodistribution studies to assess a possible effect on the availability of THIOMAB-TCO to react with ^{111}In -DOTA-Tz.

Conclusions

New conjugation methods leading to the formation of homogeneous and stable antibody conjugates are still required for pretargeted imaging applications. To our knowledge, this work represents the first maleimide-free methodology for site-specific antibody conjugation of the IEDDA pair for *in vivo* pretargeted imaging. The IEDDA-functionalized carbonylacrylic derivative proved to be a suitable alternative to the available methods for antibody fluorescence labelling and radiolabelling. This approach is particularly relevant in labelling strategies that require higher temperatures, as is often the case of those involving trivalent radiometals and macrocyclic chelators. By radiolabelling one IEDDA reagent followed by click reaction with an antibody modified in a site-specific way with the corresponding IEDDA partner, this approach allows to perform room-temperature radiolabelling more rapidly and in higher yield, compared with the traditional “one-pot” methods. Biodistribution results clearly indicate *in vivo* IEDDA reaction, but optimization is required to improve tumor uptake and tumor-to-background ratios for *in vivo* imaging.

Materials and Methods

General Information

The antibody THIOMAB™ LC-V205C was provided by Genentech (South San Francisco, CA, USA). The compound 2,2',2''-(10-(2-((4-(1,2,4,5-Tetrazin-3-yl)benzyl)amino)-2-oxoethyl)-1,4,7,10-tetraazacyclododecane-1,4,7-triyl)tri-acetic acid (DOTA-Tz) was synthesized as described by D'Onofrio *et al.*³⁷. All reagents and solvents used in chemical synthesis were of reagent grade and used without purification. General reagents were purchased from either Sigma-Aldrich or Alfa-Aesar, unless otherwise stated. All cell culture reagents were from Gibco, unless otherwise stated. Analytical thin-layer chromatography (TLC) was carried out on silica gel-coated aluminum plates with fluorescent indicator F254 (Merck). Compounds were detected with UV light ($\lambda = 254$ nm), ninhydrin or potassium permanganate. Compound purification by column chromatography was performed using high-purity grade silica gel (Merck grade 9385) with a pore size of 60 Å and 230-400 mesh particle size.

NMR spectroscopy. ¹H and ¹³C nuclear magnetic resonance (NMR) spectra were recorded on a 400 MHz DPX-400 Dual Spectrometer (Bruker) in CDCl₃, CD₃OD, or DMSO-d₆. ¹H and ¹³C chemical shifts (δ) are reported in parts per million (ppm) and referenced using the residual solvent resonances relative to tetramethylsilane. Signal multiplicity is described using the following abbreviations: s (singlet), bs (broad singlet), d (doublet), t (triplet), and m (multiplet). Characterization of the compounds is described in the SI.

Liquid chromatography-mass spectrometry. High-resolution mass determination of small molecules was performed on a Waters LCT Premier spectrometer using ESI ionisation and a TOF mass analyser. 50% (v/v) acetonitrile in bidistilled water with 0.25% (v/v) formic acid was used as mobile phase. LC-MS analysis of small molecules was performed on a Waters SQD2 with Waters H-Class UPLC using ESI ionisation (pos/neg switching). Separation was based on a Waters Acquity UPLC BEH C18 column (2.1 x 50 mm, 130 Å pore size, 1.7 μ m particle size, 0.5 mL/min flow rate, column temperature 37 °C, UV 190-400 nm), using 0.1% (v/v) formic acid in bidistilled water (solvent A) and acetonitrile (solvent B) as mobile phases. Linear gradients of solvents A and B were applied according to the following method: 0-5 min (5-100% B), 5-6.5 min (100% B) and 6.5-8 min (5% B). Protein LC-MS was performed on a Waters Acquity UPLC system equipped with a single quadrupole mass detector. Separation was based on a Waters Acquity Q6 UPLC BEH 300 C4 column (2.1 x 50 mm, 300 Å pore size, 1.7 μ m particle size, 0.2 mL/min flow rate). Solvents A (0.1% (v/v) formic acid in bidistilled water) and B (71:29:0.075 (v:v) of acetonitrile:bidistilled water:formic acid) were used as mobile phases. The gradient of solvents

A and B were applied according to the following method: 0-12 min (28-71.2% A), 12-13 min (71.2-100% A), 13-16 min (100% A), 16-16.5 min (100-28% A), and 16.5-20 min (28% A). The electrospray source was operated with a capillary voltage of 3.0 kV and a cone voltage of 20 V. Nitrogen was used as the desolvation gas at a total flow of 800 L/h with cone volume at 1 L/h. Desolvation temperature was set to 400 °C. Total mass spectra were reconstructed from the ion series using the MaxEnt algorithm preinstalled on MassLynx software (version 4.1 from Waters). To obtain the ion series described, the protein peak(s) of the chromatogram were selected for integration and further analysis.

Radio HPLC analysis. Radio reversed phase-high performance liquid chromatography (RP-HPLC) analyses were performed on a PerkinElmer Series 200 LC pump (PerkinElmer) coupled to an ultraviolet/visible (UV/VIS) detector (Shimadzu SPD-10AV) and to a γ -detector (Berthold-LB 509, Berthold Technologies). Compounds were separated using a Macherey-Nagel EC250/4 Nucleosil 100-10 C18 column (250 x 4 mm, 10 Å pore size, 10 μ m particle size, 1.0 mL/min flow rate). Linear gradients of eluent A (0.1% (v/v) TFA in bidistilled water) and eluent B (0.1% (v/v) TFA in acetonitrile) were applied according to the following method: 0-5 min (5% B), 5-25 min (5-100% B), 25-26 min (5% B), and 26-30 min (5% B). Elution was monitored *via* absorbance at 220 nm or γ -detection.

Antibody labelling was monitored by iTLC, using 12.0 x 1.0 cm strips of glass microfiber chromatography paper impregnated with silica gel (Agilent Technologies, Santa Clara, CA, USA) as stationary phase, and 30% (v/v) methanol in bidistilled water as mobile phase. Activity was detected using the γ -miniGITA TLC scanner (Elysia-raytest). GINA-Star TLC software (Elysia-raytest) allowed for data acquisition and evaluation.

Size exclusion-HPLC (SE-HPLC) analyses were performed on a PerkinElmer Flexar UHPLC System (PerkinElmer) coupled to a Gabi Nova γ -detector (Elysia-raytest). Compounds were separated using a Waters XBridge™ Protein BEH SEC column (300 x 7.8 mm, 200 Å pore size, 3.5 μ m particle size, 0.7 mL/min flow rate). Isocratic elution was performed using 0.1 M phosphate buffer pH 6.5 as mobile phase. Elution was monitored *via* absorbance at 220/280 nm or γ detection.

Cell lines and culture conditions. SK-BR-3 (HER2+) and MDA-MB-231 (HER2-) cells were obtained from the American Type Culture Collection (ATCC®, HTB-30™ and HTB-26™, respectively). Cells were grown in plastic culture flasks) at 37 °C in a humidified atmosphere of 5% CO₂. SK-BR-3 cells were cultured in McCoy's 5a Medium Modified and MDA-MB-231 cells in Dulbecco's Modified Eagle's Me-

dium (DMEM), both supplemented with 10% heat-inactivated FBS and 1% penicillin/streptomycin. A subcultivation ratio of 1:2 was adopted to SK-BR-3 cells and 1:6 to MDA-MB-231 cells.

Antibody bioconjugation. Bioconjugation reactions proceeded as follows: 25 equiv. of **CA-TCO** in DMF (5%) were added to a 13 μM THIOMAB solution in Tris-HCl buffer (20 mM, pH 8.0) and allowed to react for 2 h at 37 °C with shaking (500 rpm). An aliquot was removed and 20 equiv. of TCEP in Tris-HCl buffer (20 mM, pH 8.0) were added for 10 min at room temperature (RT) with shaking (500 rpm). The mixture was centrifuged at 16,900 g for 2 min and analysed by LC-MS. For the confocal microscopy and flow cytometry studies, the antibody was dialysed for 18-20 h at 4 °C, using a Slide-A-Lyzer™ MINI Dialysis Device with a 10K molecular weight cut-off in Tris-HCl buffer (20 mM, pH 8.0) with at least one buffer exchange. For the radiolabelling and cellular uptake studies, the antibody was purified by ultrafiltration using Amicon® Ultra-0.5 centrifugal filter devices with a 50K molecular weight cut-off, according to the manufacturer's protocol.

Click reaction with fluorescent tetrazine. 30 equiv. of 6-methyl-tetrazine-sulfo-Cy3 (Jena Biosciences) in H₂O were added to a 13 μM solution of THIOMAB-TCO in Tris-HCl buffer (20 mM, pH 8.0). The reaction was incubated for 30 min at 37 °C with shaking (500 rpm).

Sodium dodecyl sulfate-polyacrylamide gel electrophoresis. SDS-PAGE analysis was performed under reducing conditions. Samples were diluted in 4x NuPAGE LDS Sample Buffer (ThermoFisher Scientific) and 2-mercaptoethanol was added as reducing agent (10x solution). Samples were heated at 95 °C for 10 min, and loaded to a NuPAGE Bis-Tris gel (4-12% gradient). Electrophoresis proceeded at 200 V in 1x SDS Running Buffer (20x NuPAGE MES SDS Running Buffer pH 7.3). The gel was stained overnight at RT with a 0.5% (v/v) SYPRO® Ruby solution for protein detection. Fluorescence was detected in a Amersham Typhoon™ imager (GE Healthcare Life Sciences).

Confocal microscopy. Microscopy studies were performed on μ -Slide 8-well polymer coverslips chamberslides. SK-BR-3 and MDA-MB-231 cells were harvested with 1x TrypLE Express Enzyme, seeded at a density of 3.0×10^4 cells per well in complete culture medium, and allowed to adhere overnight at 37 °C and 5% CO₂. On the following day, culture medium was removed and cells were incubated for 45 min at 37 °C with THIOMAB or THIOMAB-TCO (0.75 μM) in complete medium. After antibody incubation, medium was removed, cells were washed with fresh medium, and incubated for 30 min at 37 °C with 6-methyl-tetrazine-sulfo-Cy3 solution in complete medium (29 μM - 38.5 equiv.). After tetrazine incubation, cells were washed two times with

PBS, and Hoechst 33342 (10 $\mu\text{g}/\text{mL}$) was added for 5 min at RT. Cells were then washed three times with PBS, and fixed with 4% paraformaldehyde in PBS for 15 min at RT. Cells were further washed two times with PBS, and covered in mounting medium. Blocking studies were performed in SK-BR-3 cells by pre-incubating cells with THIOMAB (0.75 μM in complete medium) before treatment with THIOMAB-TCO. Fluorescence microscopy was performed using a Zeiss LSM 880 inverted microscope, using 405 nm laser excitation for Hoechst and 488 nm laser excitation for Cy3. Identical image acquisition settings were used for experimental, control, and blocking data sets. Data was analysed using the Fiji-ImageJ software.

Flow cytometry. SK-BR-3 and MDA-MB-231 cells were harvested with TrypLE Express Enzyme, and 5.0×10^5 cells were collected, pelleted by centrifugation, and resuspended in a solution of THIOMAB or THIOMAB-TCO (0.75 μM in 3% (w/v) BSA/PBS). After 45 min at RT, cells were pelleted, washed two times with 3% BSA/PBS, and resuspended in 6-methyl-tetrazine-Sulfo-Cy3 solution in 3% BSA/PBS (29 μM - 38.5 equiv.). After 30 min at 37 °C in the dark, cells were pelleted, washed two times with 3% BSA/PBS, and resuspended in 1% (w/v) BSA/PBS containing 5 mM EDTA. All centrifugation steps were performed at 300 g for 5 min. Blocking studies were performed in SK-BR-3 cells by pre-incubating cells with THIOMAB (0.75 μM in 3% BSA/PBS) for 45 min at RT before incubation with THIOMAB-TCO. A negative, unstained control was included for each cell line to determine the level of intrinsic cell autofluorescence. Acquisition was performed on a BD Accuri™ C6 flow cytometer (BD Biosciences) set up with a 488 nm laser and the tetramethylrhodamine filter. Only results for single-cell events are shown. Data was analysed using the FlowJo X 10 software.

Radiolabelling studies. Labelling of DOTA-Tz with In-111 was performed as follows: to a vial already containing 7.4 to 30 MBq of ¹¹¹InCl₃ (Curium), DOTA-Tz to a final concentration of 1×10^{-4} M, in 0.1 M ammonium acetate buffer pH 7, followed by incubation at 80 °C for 15 min. The resulting labelling yields were between 61 and 85%. ¹¹¹In-DOTA-Tz was purified by RP-HPLC and recovered in 0.1 M phosphate buffer pH 8 and obtained with > 95% of radiochemical purity (RCP), as assessed by RP-HPLC and iTLC. The radiochemical yield (RCY) was between 44 and 56%. Activities were measured in a dose calibrator (Capintec CRC®-55tW, Mirion Technologies).

Labelling of TCO-modified THIOMAB with ¹¹¹In was accomplished through reaction of THIOMAB-TCO (13 μM) in Tris-HCl buffer (20 mM, pH 8.0) with the purified ¹¹¹In-DOTA-Tz (~ 7.4 MBq) at 37 °C. The reaction was monitored by iTLC, γ -detection. The clicked antibody conjugate was purified by

ultrafiltration using Amicon® Ultra-0.5 centrifugal filter devices with a 50K molecular weight cut-off, according to the manufacturer's protocol (final solution in 20 mM Tris-HCl buffer pH 8.0).

In vitro stability of ¹¹¹In-labelled antibody. Stability studies were performed in cell culture medium (DMEM + 10% FBS) and human serum. In addition, transchelation was assessed in the presence of an excess of diethylenetriamine-pentaacetic acid (DTPA) (0.1 M solution in ammonium acetate buffer pH 5). In general, the radiolabelled antibody was incubated at 37 °C with a 5-fold volume of each solution. Aliquots were removed at different time points and analysed by iTLC. Data were expressed as percentage of activity associated to clicked antibody at a given time point normalized to the activity associated to clicked antibody at 0 h of incubation.

Radioactive cellular uptake studies. Cellular uptake studies were performed in 24-well tissue culture plates with SK-BR-3 and MDA-MB-231 cells seeded, respectively, at a density of 2.0×10^5 and 1.25×10^5 cells per well in complete culture medium. The assays were performed on the following day. For the cellular uptake of ¹¹¹In-labelled antibody, on the day of the assay, cell medium was removed and cells were incubated with ¹¹¹In-DOTA-Tz-TCO-THIOMAB in complete medium (~ 18.5 kBq in 500 µL per well) at 37 °C. The medium containing the radioactive antibody was removed at different time points, and cells were washed twice with ice-cold PBS and lysed with 1 M NaOH for 10 min at 37°C. For the cellular uptake with pretargeting strategy, on the day of the assay, cell medium was removed and cells were incubated with THIOMAB-TCO (25nM) in complete medium for 45 min at 37 °C. Cells were washed with medium and incubated with ¹¹¹In-DOTA-Tz in complete medium (~ 18.5 kBq in 500 µL per well). At different time points, the medium containing the radioactive tetrazine was removed, and cells were washed twice with ice-cold PBS and lysed with 1 M NaOH for 10 min at 37 °C. Cellular uptake of the radiolabelled tetrazine was assessed by cell incubation with ¹¹¹In-DOTA-Tz only. Blocking studies were also performed by previous incubation with non-modified THIOMAB (25nM) in complete medium for 45 min at 37°C. In the end the experiment, radioactivity added to the cells and in the lysates was measured in a γ-counter (Berthold-LB 211, Berthold Technologies). The assays were performed with 3-4 replicates for each time point. Cellular uptake values were expressed as a percentage of total activity added to cells normalized per million of cells ± standard deviation. Statistical analysis was performed with *t*-test for the clicked antibody and with two-way ANOVA for the pretargeting strategy, with *p*-value <0.05 considered as the level of statistical significance in both cases.

In vivo studies. The animal studies were executed in laboratory animal facilities under the supervision of researchers accredited by the National Authorities and with the research project approved by the local ethical committee and the National Authority. Experiments were performed in compliance with the National and European Union directives regarding ethics, care, and protection of animals used for experimental and other scientific purposes. Biodistribution of ¹¹¹In-DOTA-Tz following pretargeting with THIOMAB-TCO was performed in female athymic nude mice (*Foxn1^{nu}*, Charles River). Animals were housed in an aseptic environment with controlled temperature (~ 24 °C) and humidity, following a 12 h light/12 h dark schedule and maintained on a normal diet *ad libitum*. Mice were distributed in two groups for SK-BR-3 xenografts (n = 3-4) and one group for MDA-MB-231 xenografts (n = 3). Each mice (16-weeks old, ~ 28-30 g) was subcutaneously injected in the right flank with 150 µL of a 50:50 (v:v) Matrigel:FBS suspension containing ~ 10×10^6 freshly-harvested SK-BR-3 or MDA-MB-231 cells. Water supplemented with 17-β-estradiol (0.67 µg/mL) was given to animals inoculated with SK-BR-3 cells and changed 2 times per week, and an estradiol-containing pomade was also applied at the inoculation site every day. Tumor growth was determined by measurement of tumors using calipers twice a week. Volume of spheroid SK-BR-3 tumors ranged between 100 and 200 mm³ and was calculated using the formula $V = (4/3) \times \pi \times r^3$, where *r* represents the radius of the sphere. Volume of ellipsoid MDA-MB-231 tumors ranged between 500 and 700 mm³ and was calculated using the formula $V = (\pi/6) \times L \times W^2$, where *L* and *W* represent the major and minor diameters, respectively. At day 12 after inoculation, tumor-bearing mice received an intravenous (iv) injection *via* the tail vein of THIOMAB-TCO or unmodified THIOMAB (control group) at a total dose of 5 mg/kg (~ 100 µL/mouse). Animals were maintained in the temperature- and humidity-controlled room and, 24 hours later, were iv injected in the tail vein with 2.8-4.1 MBq of ¹¹¹In-DOTA-Tz (~ 100 µL/mouse). Animals were sacrificed 24 h post-injection of ¹¹¹In-labelled tetrazine (~ 48 h after antibody injection) by cervical dislocation. The ID in the mouse and the activity remaining in the sacrificed animal were measured in a dose calibrator (Capintec CRC®-55tW, Mirion Technologies), and the difference was assumed to be due to excretion. Tissues and organs of interest were dissected, rinsed to remove excess blood, weighted, and the activity measured in a γ-counter (Berthold-LB 211, Berthold Technologies). Tissue and organ uptakes were expressed as percentage of ID per gram of tissue or organ (% ID/g). For blood, bone, and muscle, the percentage of ID/g was estimated assuming that these tissues represent, respectively, 6, 10, and 40% of the total body weight. Statistical analysis was performed with two-way ANOVA, with *p*-value <0.05 considered as the level of statistical significance.

ASSOCIATED CONTENT

Supporting Information

The Supporting Information with experimental and additional figures is available free of charge on the ACS Publications website.

AUTHOR INFORMATION

Corresponding Authors

Filipa Mendes – Center for Nuclear Sciences and Technologies (C²TN), Instituto Superior Técnico, Universidade de Lisboa, Lisboa, Portugal; Departamento de Engenharia e Ciências Nucleares (DECN), Instituto Superior Técnico, Universidade de Lisboa, Lisboa, Portugal. Email: fmendes@ctn.tecnico.ulisboa.pt

Gonçalo J. L. Bernardes – Department of Chemistry, University of Cambridge, Cambridge CB2 1EW, United Kingdom; Instituto de Medicina Molecular João Lobo Antunes (iMM-JLA), Faculdade de Medicina, Universidade de Lisboa, Portugal; Email: gb453@cam.ac.uk

Bruno L. Oliveira – Instituto de Medicina Molecular João Lobo Antunes (iMM-JLA), Faculdade de Medicina, Universidade de Lisboa, Portugal; Email: bruno.oliveira@medicina.ulisboa.pt

Notes

In regard to this publication, G.J.L.B. has received research reagents from Genentech.

ACKNOWLEDGMENTS

This work is funded by Fundação para a Ciência e Tecnologia – FCT (PTDC/BTM-TEC/29256/2017 (co-funded by Lisboa2020 - EU FEDER to F.Mendes) and UID/Multi/04349/2019). V.F.C.F. also acknowledges FCT for the PhD fellowship (SFRH/BD/108623/2015) and the Federation of European Biochemical Societies for a Summer Fellowship. Funding is also acknowledged to the Royal Society (URF to G.J.L.B., URF\R\180019) and FCT Portugal (iFCT to G.J.L.B., IF/00624/2015 and FCT Stimulus to B.L.O., CEECIND/02335/2017). This project has received funding from the European Union's Horizon 2020 research and innovation programme under grant agreements Nos. 807281, 702428 and 852985. The authors would like to thank Dr Célia Fernandes (C²TN) for fruitful discussions and Elisabete Correia (C²TN) for excellent technical support.

REFERENCES

(1) Warram, J. M., de Boer, E., Sorace, A. G., Chung, T. K., Kim, H., Pleijhuis, R. G., van Dam, G. M., Rosenthal, E. L. (2014) Antibody-based imaging strategies for cancer. *Cancer Metastasis Rev.* 33 (2-3), 809-822.
(2) Dammes, N. and Peer, D. (2020) Monoclonal antibody-based molecular imaging strategies and theranostic opportunities. *Theranostics* 10 (2), 938-955.

(3) Freise, A. C., and Wu, A. M. (2015) In vivo imaging with antibodies and engineered fragments. *Mol. Immunol.* 67 (2), 142-152.
(4) Garousi, J., Orlova, A., Frejd, F. Y., Tolmachev, V. (2020) Imaging using radiolabelled targeted proteins: radioimmunodetection and beyond. *EJNMMI radiopharm. Chem.* 5 (1), 16-16.
(5) Reardan, D. T., Mearns, C. F., Goodwin, D. A., McTigue, M., David, G. S., Stone, M. R., Leung, J. P., Bartholomew, R. M., Frincke, J. M. (1985) Antibodies against metal chelates. *Nature* 316 (6025), 265-268.
(6) Hnatowich, D. J., Virzi, F., Rusckowski, M. (1987) Investigations of avidin and biotin for imaging applications. *J. Nucl. Med.* 28 (8), 1294-1302.
(7) Knight, J. C., and Cornelissen, B. (2014) Bioorthogonal chemistry: implications for pretargeted nuclear (PET/SPECT) imaging and therapy. *Nucl. Med. Mol. Imaging* 4 (2), 96-113.
(8) Altai, M., Membreno, R., Cook, B., Tolmachev, V., Zeglis, B. M. (2017) Pretargeted Imaging and Therapy. *J. Nucl. Med.* 58 (10), 1553-1559.
(9) Oliveira, B. L., Guo, Z., Bernardes, G. J. L. (2017) Inverse electron demand Diels-Alder reactions in chemical biology. *Chem. Soc. Rev.* 46 (16), 4895-4950.
(10) Devaraj, N. K. (2018) The Future of Bioorthogonal Chemistry. *ACS Cent. Sci.* 4 (8), 952-959.
(11) Rondon, A., and Degoul, F. (2020) Antibody Pretargeting Based on Bioorthogonal Click Chemistry for Cancer Imaging and Targeted Radionuclide Therapy. *Bioconjug. Chem.* 31 (2), 159-173.
(12) Blackman, M. L., Royzen, M., Fox, J. M. (2008) Tetrazine ligation: fast bioconjugation based on inverse-electron-demand Diels-Alder reactivity. *J. Am. Chem. Soc.* 130 (41), 13518-13519.
(13) Garcia, M. F., Gallazzi, F., Junqueira, M. S., Fernandez, M., Camacho, X., Mororo, J. D. S., Faria, D., Carneiro, C. G., Couto, M., Carrion, F., Pritsch, O., Chammas, R., Quinn, T., Cabral, P., Cerecetto, H. (2018) Synthesis of hydrophilic HYNIC-[1,2,4,5]tetrazine conjugates and their use in antibody pretargeting with (99m)Tc. *Org. Biomol. Chem.* 16 (29), 5275-5285.
(14) Mandikian, D., Rafidi, H.; Adhikari, P., Venkatraman, P., Nazarova, L., Fung, G., Figueroa, I., Ferl, G. Z., Ulufatu, S., Ho, J.; McCaughey, C., Lau, J., Yu, S. F., Prabhu, S., Sadowsky, J., Boswell, C. A. (2018) Site-specific conjugation allows modulation of click reaction stoichiometry for pretargeted SPECT imaging. *MAbs* 10 (8), 1269-1280.
(15) Rossin, R., Verkerk, P. R., van den Bosch, S. M., Vulders, R. C., Verel, I.; Lub, J., Robillard, M. S. (2010) In vivo chemistry for pretargeted tumor imaging in live mice. *Angew. Chem. Int. Ed. Engl.* 49 (19), 3375-3378.
(16) Zeglis, B. M., Sevak, K. K., Reiner, T., Mohindra, P., Carlin, S. D., Zanzonico, P., Weissleder, R., Lewis, J. S. (2013) A pretargeted PET imaging strategy based on bioorthogonal Diels-Alder click chemistry. *J. Nucl. Med.* 54 (8), 1389-1396.
(17) Houghton, J. L., Zeglis, B. M., Abdel-Atti, D., Sawada, R., Scholz, W. W., Lewis, J. S. (2016) Pretargeted Immuno-PET of Pancreatic Cancer: Overcoming Circulating Antigen and Internalized Antibody to Reduce Radiation Doses. *J. Nucl. Med.* 57 (3), 453-459.
(18) Cook, B. E., Adumeau, P., Membreno, R., Carnazza, K. E., Brand, C., Reiner, T., Agnew, B. J., Lewis, J. S., Zeglis, B. M. (2016) Pretargeted PET Imaging Using a Site-Specifically Labeled Immunoconjugate. *Bioconjugate Chem.* 27 (8), 1789-1795.
(19) Billaud, E. M. F., Belderbos, S., Cleeren, F., Maes, W., Van de Wouwer, M., Koole, M., Verbruggen, A., Himmelreich, U., Geukens, N., Bormans, G. (2017) Pretargeted PET Imaging Using a

- Bioorthogonal (18)F-Labeled trans-Cyclooctene in an Ovarian Carcinoma Model. *Bioconjug. Chem.* 28 (12), 2915-2920.
- (20) Keinanen, O., Fung, K., Pourat, J., Jallinoja, V., Vivier, D., Pillarsetty, N. K., Airaksinen, A. J., Lewis, J. S., Zeglis, B. M., Sarparanta, M. (2017) Pretargeting of internalizing trastuzumab and cetuximab with a (18)F-tetrazine tracer in xenograft models. *EJNMMI Res.* 7 (1), 95-98.
- (21) Ruivo, E., Elvas, F., Adhikari, K., Vangestel, C., Van Haesendonck, G., Lemiere, F., Staelens, S., Stroobants, S., Van der Veken, P., Wyffels, L., Augustyns, K. (2020) Preclinical Evaluation of a Novel (18)F-Labeled dTCO-Amide Derivative for Bioorthogonal Pretargeted Positron Emission Tomography Imaging. *ACS Omega* 5 (9), 4449-4456.
- (22) Evans, H. L., Nguyen, Q. D., Carroll, L. S., Kaliszczak, M., Twyman, F. J., Spivey, A. C., Aboagye, E. O. (2014) A bioorthogonal (68)Ga-labelling strategy for rapid in vivo imaging. *Chem. Commun.* 50 (67), 9557-9560.
- (23) Meyer, J.-P., Houghton, J. L., Kozlowski, P., Abdel-Atti, D., Reiner, T., Pillarsetty, N. V. K., Scholz, W. W., Zeglis, B. M., Lewis, J. S. (2016) 18F-Based Pretargeted PET Imaging Based on Bioorthogonal Diels-Alder Click Chemistry. *Bioconjug. Chem.* 27 (2), 298-301.
- (24) Edem, P. E., Jorgensen, J. T., Norregaard, K., Rossin, R., Yazdani, A., Valliant, J. F., Robillard, M., Herth, M. M., Kjaer, A. (2020) Evaluation of a (68)Ga-Labeled DOTA-Tetrazine as a PET Alternative to (111)In-SPECT Pretargeted Imaging. *Molecules* 25 (3), 463-477.
- (25) Hoyt, E. A., Cal, P. M. S. D., Oliveira, B. L., Bernardes, G. J. L. (2019) Contemporary approaches to site-selective protein modification. *Nature Rev. Chem.* 3, 147-171.
- (26) Chalker, J. M., Bernardes, G. J., Lin, Y. A., Davis, B. G. (2009) Chemical modification of proteins at cysteine: opportunities in chemistry and biology. *Chem. Asian J.* 4 (5), 630-640.
- (27) Ochtrop, P., and Hackenberger, C. P. R. (2020) Recent advances of thiol-selective bioconjugation reactions. *Curr. Opin. Chem. Biol.* 58, 28-36.
- (28) Baldwin, A. D., and Kiick, K. L. (2011) Tunable Degradation of Maleimide-Thiol Adducts in Reducing Environments. *Bioconjug. Chem.* 22 (10), 1946-1953.
- (29) Cal, P. M., Bernardes, G. J., Gois, P. M. (2014) Cysteine-selective reactions for antibody conjugation. *Angew. Chem. Int. Ed. Engl.* 53 (40), 10585-10587.
- (30) Ravasco, J. M. J. M., Faustino, H., Trindade, A., Gois, P. M. P. (2019) Bioconjugation with Maleimides: A Useful Tool for Chemical Biology. *Chem. Eur. J.* 25 (1), 43-59.
- (31) Bernardim, B., Cal, P. M., Matos, M. J., Oliveira, B. L., Martinez-Saez, N., Albuquerque, I. S., Perkins, E., Corzana, F., Burtoloso, A. C., Jimenez-Oses, G., Bernardes, G. J. (2016) Stoichiometric and irreversible cysteine-selective protein modification using carbonylacrylic reagents. *Nat. Commun.* 7, 13128-13132.
- (32) Bernardim, B., Matos, M. J., Ferhati, X., Compañón, I., Guerreiro, A., Akkapeddi, P., Burtoloso, A. C. B., Jiménez-Osés, G., Corzana, F., Bernardes, G. J. L. (2019) Efficient and irreversible antibody-cysteine bioconjugation using carbonylacrylic reagents. *Nat. Protoc.* 14 (1), 86-99.
- (33) Junutula, J. R., Raab, H., Clark, S., Bhakta, S., Leipold, D. D., Weir, S., Chen, Y., Simpson, M., Tsai, S. P., Dennis, et al. (2008) Site-specific conjugation of a cytotoxic drug to an antibody improves the therapeutic index. *Nat. Biotechnol.* 26 (8), 925-932.
- (34) Dijkers, E. C., Oude Munnink, T. H., Kosterink, J. G., Brouwers, A. H., Jager, P. L., de Jong, J. R., van Dongen, G. A., Schröder, C. P., Lub-de Hooge, M. N., de Vries, E. G. (2010) Biodistribution of 89Zr-trastuzumab and PET Imaging of HER2-Positive Lesions in Patients With Metastatic Breast Cancer. *Clin. Pharmacol. Ther.* 87 (5), 586-592.
- (35) Holloway, C. M. B., Scollard, D. A., Caldwell, C. B., Ehrlich, L., Kahn, H. J., Reilly, R. M. (2013) Phase I trial of intraoperative detection of tumor margins in patients with HER2-positive carcinoma of the breast following administration of 111In-DTPA-trastuzumab Fab fragments. *Nucl. Med. Biol.* 40 (5), 630-637.
- (36) Sandstrom, M., Lindskog, K., Velikyan, I., Wennborg, A., Feldwisch, J., Sandberg, D., Tolmachev, V., Orlova, A., Sorensen, J., Carlsson, J., Lindman, H., Lubberink, M. (2016) Biodistribution and Radiation Dosimetry of the Anti-HER2 Affibody Molecule 68Ga-ABY-025 in Breast Cancer Patients. *J. Nucl. Med.* 57 (6), 867-71.
- (37) Ulaner, G. A., Lyashchenko, S. K., Riedl, C., Ruan, S., Zanzonico, P. B., Lake, D., Jhaveri, K., Zeglis, B., Lewis, J. S., O'Donoghue, J. A. (2018) First-in-Human Human Epidermal Growth Factor Receptor 2-Targeted Imaging Using (89)Zr-Pertuzumab PET/CT: Dosimetry and Clinical Application in Patients with Breast Cancer. *J. Nucl. Med.* 59 (6), 900-906.
- (38) Pereira, P. M. R., Abma, L., Henry, K. E., Lewis, J. S. (2018) Imaging of human epidermal growth factor receptors for patient selection and response monitoring - From PET imaging and beyond. *Cancer Lett.* 419, 139-151.
- (39) Nazarova, L., Rafidi, H., Mandikian, D., Ferl, G. Z., Koerber, J. T., Davies, C. W., Ulufatu, S.; Ho, J., Lau, J., Yu, S. F., Ernst, J., Sadowsky, J. D., Boswell, C. A. (2020) Effect of Modulating FcRn Binding on Direct and Pretargeted Tumor Uptake of Full-length Antibodies. *Mol. Cancer Ther.* 19 (4), 1052-1058.
- (40) Mandleywala, K., Shmuel, S., Pereira, P. M. R., Lewis, J. S. (2020) Antibody-Targeted Imaging of Gastric Cancer. *Molecules* 25 (20), 4621-4633.
- (41) Ren, W., Liu, Y., Wan, S., Fei, C., Wang, W., Chen, Y., Zhang, Z., Wang, T., Wang, J., Zhou, L., Weng, Y., He, T., Zhang, Y. (2014) BMP9 Inhibits Proliferation and Metastasis of HER2-Positive SK-BR-3 Breast Cancer Cells through ERK1/2 and PI3K/AKT Pathways. *Plos One* 9 (5), e96816.
- (42) D'Onofrio, A., Paulo, A., Gano, L., Oliveira, C., Mendes, F., Dunn, S., Fierle, J. (2018) Towards clickable radioimmunoconjugates as theranostic agents for TEM1 targeting. *Mol. Imag. Biol.* 20, S1, 1-584.
- (43) Austin, C. D., De Maziere, A. M., Pisacane, P. I., van Dijk, S. M., Eigenbrot, C., Sliwkowski, M. X., Klumperman, J., Scheller, R. H. (2004) Endocytosis and sorting of ErbB2 and the site of action of cancer therapeutics trastuzumab and geldanamycin. *Mol. Biol. Cell* 15 (12), 5268-82.
- (44) Ram, S., Kim, D., Ober, R. J., Ward, E. S. (2014) The level of HER2 expression is a predictor of antibody-HER2 trafficking behavior in cancer cells. *MAbs* 6 (5), 1211-1219.
- (45) Ovacik, M., and Lin, K. (2018) Tutorial on Monoclonal Antibody Pharmacokinetics and Its Considerations in Early Development. *Clin. Transl. Sci.* 11 (6), 540-552.
- (46) Rossin, R., Läppchen, T., van den Bosch, S. M., Laforest, R., Robillard, M. S. (2013) Diels-Alder Reaction for Tumor Pretargeting: In Vivo Chemistry Can Boost Tumor Radiation Dose Compared with Directly Labeled Antibody. *J. Nucl. Med.* 54, (11) 1989-1995.
- (47) Meyer, J.-P., Tully, K. M., Jackson, J., Dilling, T. R., Reiner, T., Lewis, J. S. (2018) Bioorthogonal Masking of Circulating Antibody-TCO Groups Using Tetrazine-Functionalized Dextran Polymers. *Bioconjug. Chem.* 29 (2), 538-545.
- (48) Pereira, P. M. R., Sharma, S. K., Carter, L. M., Edwards, K. J., Pourat, J., Ragupathi, A., Janjigian, Y. Y., Durack, J. C., Lewis, J. S.

(2018) Caveolin-1 mediates cellular distribution of HER2 and affects trastuzumab binding and therapeutic efficacy. *Nat. Commun.* 9 (1), 5137-5151.

(49) Pereira, P. M. R., Mandleywala, K., Ragupathi, A., Carter, L. M., Goos, J, Janjigian, Y. Y., Lewis, J. S. (2019) Temporal Modulation of HER2 Membrane Availability Increases Pertuzumab Uptake and Pretargeted Molecular Imaging of Gastric Tumors. *J. Nucl. Med.* 60 (11), 1569-1578.

(50) Hommelgaard, A. M., Lerdrup, M., van Deurs, B. (2004) Association with membrane protrusions makes ErbB2 an internalization-resistant receptor. *Mol. Bio. Cell* 15 (4), 1557-1567.

(51) Pereira, P. M. R., Mandleywala, K., Ragupathi, A., Lewis, J. S. (2020) Acute Statin Treatment Improves Antibody Accumulation in EGFR- and PSMA-Expressing Tumors. *Clin. Cancer Res.* DOI: 10.1158/1078-0432.ccr-20-1960.

